



n-Hexadecane hydroisomerization over Pt-HBEA catalysts. Quantification and effect of the intimacy between metal and protonic sites



N. Batalha^{a,*}, L. Pinard^{a,*}, C. Bouchy^b, E. Guillon^b, M. Guisnet^{c,d,*}

^a IC2MP, UMR 7285, Université de Poitiers, 4 rue Michel Brunet, 86022 Poitiers, France

^b IFP Energies Nouvelles, Rond-point de l'échangeur de Solaize, BP3, 69360 Solaize, France

^c University of Poitiers, 40 avenue Recteur Pineau, 86022 Poitiers Cedex, France

^d Instituto Superior Tecnico (UTL), Av. Rovisco Pais, 1096 Lisboa Codex, Portugal

ARTICLE INFO

Article history:

Received 11 March 2013

Revised 11 July 2013

Accepted 16 July 2013

Keywords:

Bifunctional catalysis

Pt-HBEA zeolite catalysts

n-Hexadecane hydroisomerization

Metal-acid balance

Intimacy criterion

ABSTRACT

n-Hexadecane (*n*-C₁₆) transformation was carried out at 220 °C and 30 bar over bifunctional catalysts with Pt and HBEA as hydro-dehydrogenating and acid components. Three series of catalysts were prepared, with different levels of proximity between Pt and acid sites: in series 1, Pt was essentially located on the outer surface of HBEA crystal agglomerates of ~12.5 μm, series 2 and 3 resulted from combination of Pt-Al₂O₃ and HBEA particles of ~70 μm and from mechanical mixture of Pt-Al₂O₃ and HBEA particles of ~300 μm, respectively. The rate and selectivity of *n*-C₁₆ hydroisomerization was shown to be determined by only two parameters, the balance between the metal and acid functions and their degree of intimacy. Both of them were easy to be quantified: the first one by the C_{Pt}/C_{H^+} ratio between the concentrations of accessible Pt and protonic sites, the second one by n_{as} , the number of acid steps undergone by olefinic intermediates during their diffusion between two Pt sites which can be drawn from the initial product distribution.

© 2013 Elsevier Inc. All rights reserved.

1. Introduction

Selective *n*-alkane hydroisomerization is the desired reaction in two major refining processes: C₅–C₆ hydroisomerization that generates high octane for the gasoline pool while contributing no undesired olefins or aromatics [1] and dewaxing of base oils and diesel fuels, the aim of which is to improve their cold flow properties by selective isomerization of long-chain *n*-alkane feed components [2,3]. Both processes involve bifunctional catalysts with Pt and H zeolite as hydrogenating and acid components.

The scheme of bifunctional catalysis and especially that of *n*-alkane hydroisomerization was established more than 50 years ago [4]. Seven successive steps are required: 3 chemical ones, dehydrogenation on the Pt sites of *n*-alkane molecules into *n*-alkenes, isomerization over the acid sites of *n*-alkenes into isoalkenes, and hydrogenation of these isoalkenes, and 4 physical steps, i.e., diffusion of *n*-alkane molecules from the gas phase to the Pt sites, diffusion of *n*-alkenes from the Pt to the acid

sites, diffusion of isoalkenes from the acid to the Pt sites, lastly diffusion of isoalkanes from the Pt sites to the gas phase. The requirements as well as the implications of the bifunctional reaction scheme were experimentally demonstrated in many works [3–10].

Nevertheless, several authors have proposed an alternative explanation [11–14], considering that the bifunctional hydroisomerization scheme could not account for some catalytic data, part of them being obtained with Pt–H zeolite catalysts. In this explanation (hydrogen spillover), the only function of the metal was to provide H atoms (and not alkenes) to the acid support, these H atoms promoting the carbenium ions desorption from the protonic sites. However, a recent review paper [15] rejects this hydrogen spillover mechanism over Pt supported on H zeolite catalysts and more generally on acidic non-reducible metal oxides, namely on the basis of a misinterpretation of the hydroisomerization bifunctional scheme.

The hydroisomerization of *n*-alkanes over Pt-HFAU zeolites was investigated by several groups, the focus being placed either on the reaction scheme over a chosen catalyst [5,6,16–20] or on the change in rate and reaction scheme with the characteristics of the hydrogenating and acid functions (especially with the balance between these functions) [21–24]. Note moreover that in most of the studies, only qualitative data of this balance effect were

* Corresponding authors. Address: University of Poitiers, 40 avenue Recteur Pineau, 86022 Poitiers Cedex, France. Fax: +33 (0) 5 49 45 37 74 (M. Guisnet).

E-mail addresses: ludovic.pinard@univ-poitiers.fr (L. Pinard), michel.guisnet@univ-poitiers.fr (M. Guisnet).

presented. The first tentative of quantification was made in *n*-heptane [21,22] and *n*-decane hydroisomerization [23] on a series of PtUSHY catalysts differing by their Pt content (from 0.07 to 1.5 wt%); the C_{Pt}/C_A ratio between the concentrations of accessible Pt and acid sites on which the heat of NH_3 adsorption was greater than 100 kJ mol^{-1} was chosen to quantitatively express this balance [21–23]. The activity, stability, and selectivity of the catalysts were shown to be definitely governed by the C_{Pt}/C_A ratio. Thus, the activity per acid site first increased at low values of this ratio then became constant, in agreement with the change in the rate limiting reaction: from hydro-dehydrogenation over Pt sites at low values, to skeletal rearrangement or cracking of olefinic intermediates over acid sites at high values. Furthermore, both stability and selectivity to isomers increased with C_{Pt}/C_A up to their optimal values. However, the observation that optimal stability and selectivity required C_{Pt}/C_A values higher than those necessary for the optimal activity suggested the effect of an additional parameter, which was proposed to be the number of acid sites encountered by the olefinic intermediates during their diffusion between two Pt sites [21–23]. It should be remarked that this number should be significantly dependent on the degree of intimacy between Pt and acid sites; however, no quantification of this number was proposed.

Lastly, no diffusion limitations within the micropores of this tridimensional large pore zeolite could be generally detected, contrary to what was observed when Pt was supported over monodimensional large pore zeolites such as HMOR [24], tridimensional medium H zeolites such as HMF1 [24–27] and monodimensional medium H zeolites such as HTON [28–30] with, in this last case, a fast blockage by carbonaceous deposits of the access to the inner acid sites [31].

The first aim of this work is to confirm the main conclusion drawn from *n*-C₇ and *n*-C₁₀ hydroisomerization over PtUSHY catalysts [21–24], i.e., that the characteristics (activity, stability, and selectivity) of bifunctional catalysts with Pt and a tridimensional large pore zeolite as hydrogenating and acid components, depend essentially (and probably only) on two of their physicochemical characteristics: the balance and the degree of intimacy between their hydrogenating and acid functions. In addition, to quantitatively express the effect of these two characteristics, representative parameters easy to be quantified are proposed: (i) for representing more accurately the hydrogenating/acid balance, the C_{Pt}/C_{H^+} ratio between the concentrations of accessible Pt and protonic sites (known to be the acid sites active in the olefinic intermediates rearrangement and cracking) was substituted for the C_{Pt}/C_A ratio used in previous works; (ii) the average number of acid steps (n_{as}) involved in the apparent formation of one product molecule from *n*-C₁₆ which can be estimated from the product composition was proposed for expressing the intimacy between hydrogenating and acid functions. The effect of these quantitative parameters was established in *n*-C₁₆ hydroisomerization over three different series of Pt-HBEA catalysts differing significantly by the degree of intimacy between hydrogenating and acid sites, the HBEA zeolite being chosen because of its tridimensional large micropores and of its well-known high activity.

2. Experimental

2.1. Preparation and characterizations of the bifunctional catalysts

Three series of bifunctional catalysts were prepared from a HBEA sample supplied by PQ Corporation (Fig. 1). The characteristics of this zeolite sample were the following: agglomerates ($\sim 12.5 \mu\text{m}$) of crystallites [32] with an average size of 14 nm, framework Si/Al molar ratio of 15, total surface area of $740 \text{ m}^2 \text{ g}^{-1}$, micropore and mesopore volumes of 0.30 and $0.50 \text{ cm}^3 \text{ g}^{-1}$, respectively.

A series of Pt-exchanged HBEA catalysts (S1) with Pt contents from 0.2 to 1.5 wt% were prepared by ion exchange of the HBEA zeolite with $[Pt(NH_3)_4]^{2+}$ in presence of NH_4^+ competitor ions ($NH_4^+/[Pt(NH_3)_4]^{2+} = 100$), followed by calcination at 450°C for 4 h (after a T increase of 2°C/min from 110 to 450°C), then reduction under hydrogen at 300°C for 12 h. Note that the 0.2Pt/HBEA and 0.5Pt/HBEA sample were calcined under more severe conditions (T increase of 5°C/min from 110 to 450°C) so as to get larger platinum particles. Two other series of catalysts resulted from mixing of different amounts of HBEA zeolite and of 1 wt% PtA alumina sample (PtA). Gamma alumina was obtained through the calcination at 550°C for 3 h of a boehmite sample (DISPAL 23N4-80) supplied by SASOL. After calcination, the alumina presented a surface area of $218 \text{ m}^2 \text{ g}^{-1}$ and a pore volume of $0.42 \text{ cm}^3 \text{ g}^{-1}$. The alumina was impregnated via the incipient wetness technique with $H_2PtCl_6 \cdot 6H_2O$ as precursor, calcined at 500°C over dry air for 12 h and then treated at 300°C under hydrogen flow for 3 h. In the S2 series of composite catalysts, the HBEA and PtA powders were intimately mixed together, then pelletized, and sieved to 0.2–0.4 mm, whereas in the S3 series, 0.2–0.4 mm particles of PtA and HBEA were simply mixed together. The composite bifunctional catalysts were called PtA-HBEA (a–b) S2 and S3, where a and b were the wt% of PtA and HBEA, respectively.

The acidity of the HBEA zeolite and of the bifunctional catalysts of the S1 series was determined by pyridine chemisorption followed by infrared spectroscopy using the extinction coefficients reported in Ref. [33]. The dispersion of platinum was estimated by CO adsorption followed by infrared spectroscopy [34].

2.2. *n*-C₁₆ transformation

The transformation of *n*-C₁₆ (Aldrich, >99.9% purity) was carried out in a fixed-bed stainless steel reactor under the following conditions: temperature: 220°C , total pressure: 30 bar, $H_2/n\text{-C}_{16}$ molar ratio: 20 and WHSV (*n*-C₁₆ weight hourly space velocity): $2\text{--}100 \text{ h}^{-1}$. The classical tests for determining the eventual existence of external and internal (within the pores of the catalyst particles) limitations, i.e., effect on *n*-C₁₆ conversion of the change in the flow rate and catalyst amount at constant WHSV value and of the change in particle size, respectively [35], were carried out. No change in conversion could be observed, which shows the absence of mass transport limitations.

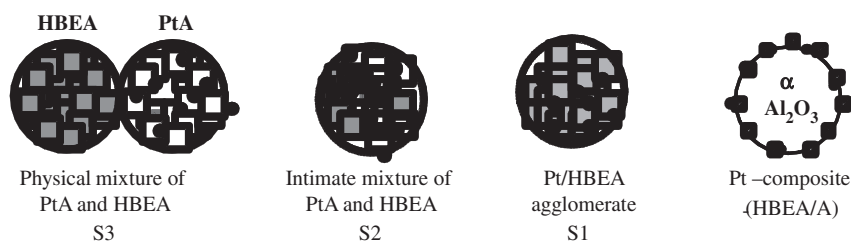


Fig. 1. Schematic presentation of the series of bifunctional Pt-HBEA catalysts.

To avoid condensation during product analysis, *n*-C₁₆ was diluted with *n*-hexane (*n*-C₆/*n*-C₁₆ ratio of 9), which was demonstrated to be inert under the operating conditions. The catalyst bed was composed of 0.3 g of catalyst with a particle size between 0.2 and 0.4 mm to avoid pressure drop in mixture with 1.7 g of Carborundum (particle size of 0.25 mm). Before reaction, all the catalysts were reduced under a hydrogen flow at 450 °C for 6 h. To obtain different conversion values, the weight hour space velocity (WHSV) was changed by modifying either the catalyst weight and/or the flow rates. The reaction products were analyzed online by GC equipped with a 50 m CPSil-5 capillary column from Chrom-pack, with hydrogen as carrier gas (13 psi) and a FID detector.

3. Results

3.1. Catalyst characteristics

The main physicochemical characteristics of all the bifunctional catalysts (series 1, 2, 3) are reported in Table 1. In addition, those of a bifunctional catalyst (0.7Pt/(HBEA/A)) prepared from nano-crystals of BEA formed by germination on an α -Al₂O₃ surface [36,37] were also indicated.

The concentration C_{H+} of the Brønsted acid sites (able to retain pyridine at 150 °C) of the HBEA zeolite was found to be equal to 440 $\mu\text{mol g}^{-1}$. The introduction of platinum in the HBEA zeolite causes a small decrease (10% at the maximum) in the protonic acidity (Table 1, series 1). Low values of the Pt dispersion

(2–18%) were found on all the Pt-exchanged HBEA catalysts (S1 series and 0.7Pt/(HBEA/A)) (Table 1). Hence, with all the samples, the average size of the corresponding Pt crystals was between ~6 and 50 nm, thus much larger than the zeolite pore opening. Therefore, it can be concluded that most of the platinum was located on the external surface of the HBEA zeolite crystals. Table 1 shows that with all these S1 catalysts, the values of the concentrations of accessible Pt sites (C_{Pt}) were much lower than those of the C_{H+} concentration. As a consequence, the values of the C_{Pt}/C_{H+} ratio, which was chosen as representative of the balance between hydrogenating and acid functions were very low: from 0.0003 to 0.032.

Furthermore, as it is well known, no protonic sites able to chemisorb pyridine can be detected over alumina (A) and C_{H+} of the PtA sample was equal to zero. On PtA, the Pt dispersion was found to be equal to 40%. For the two series of bifunctional catalysts prepared by mixture of PtA and HBEA (S2 and S3), the values of C_{Pt}, C_{H+}, and C_{Pt}/C_{H+} reported in Table 1 were calculated from the relative amounts of the components in the mixture. For these series of catalysts, the C_{Pt}/C_{H+} ranged from 0.022 to 0.134–0.17.

3.2. *n*-C₁₆ transformation

Under the operating conditions, pure HBEA and PtA samples were completely inactive, whereas all the bifunctional samples were able to catalyze *n*-hexadecane transformation and with a quasi perfect stability. The values of turnover frequency (TOF, i.e., activity per acid site) are reported in Table 2. Furthermore, the

Table 1
Physicochemical characteristics of the bifunctional catalysts: Pt dispersion (*D*) estimated by CO chemisorption, concentrations of accessible Pt atoms (C_{Pt}), of protonic sites (C_{H+}), and balance between metal and acid functions (C_{Pt}/C_{H+}).

	Catalyst	<i>D</i> ^a (%)	C _{Pt} ($\mu\text{mol g}^{-1}$)	C _{H+} ($\mu\text{mol g}^{-1}$)	C _{Pt} /C _{H+}
Series S1	HBEA	–	–	440 ^b	0
	0.7Pt/(HBEA/A)	18	4.7	86 ^b	0.055
	0.2Pt/HBEA	2	0.1	394 ^b	0.0003
	0.5Pt/HBEA	6	1.7	406 ^b	0.0040
	1.0Pt/HBEA	17	8.3	425 ^b	0.0200
	1.5Pt/HBEA	16	12.7	396 ^b	0.0320
Series S2 and S3	PtA	40	19.7	0	∞
	PtA-HBEA(5-95)	40	1.0	418 ^c	0.002
	PtA-HBEA(25-75)	40	4.9	330 ^c	0.015
	PtA-HBEA(50-50)	40	9.9	220 ^c	0.045
	PtA-HBEA(75-25)	40	14.8	110 ^c	0.130

^a Measured by CO chemisorption at 25 °C.

^b Measured by pyridine adsorption at 150 °C.

^c Calculated from the amount of zeolite in the composite catalysts.

Table 2
Values of the activity per acid site (TOF) and of the ratios between cracking and isomerization products (C/I)₀ and between the multibranched and monobranched isomers ratios (B/M)₀ estimated by extrapolation at zero conversion. Wt fractions of monobranched (M), multibranched (B) isomers, and cracking products (C) in the reaction products.

Series	Catalyst	C _{Pt} /C _{H+}	TOF (h ⁻¹)	(C/I) ₀	(B/M) ₀	wt fractions		
						M	B	C
S1	0.7Pt/(HBEA/A)	0.055	73	0	0	1	0	0
	0.2Pt/HBEA	0.0003	15	0.6	1.9	0.22	0.41	0.37
	0.5Pt/HBEA	0.0040	31	0.10	1.3	0.40	0.51	0.09
	1.0Pt/HBEA	0.020	30	0.06	1.2	0.43	0.51	0.06
	1.5Pt/HBEA	0.032	31	0.06	1.2	0.43	0.51	0.06
S2	PtA-HBEA(5-95)	0.002	14	0.73	4.1	0.11	0.46	0.42
	PtA-HBEA(25-75)	0.015	21	0.51	4.1	0.13	0.53	0.34
	PtA-HBEA(50-50)	0.045	23	0.30	3.2	0.18	0.59	0.23
	PtA-HBEA(75-25)	0.130	24	0.20	1.8	0.30	0.54	0.17
S3	PtA-HBEA(5-95)	0.002	5	0.70	3.7	0.13	0.46	0.41
	PtA-HBEA(25-75)	0.015	21	0.70	3.7	0.13	0.46	0.41
	PtA-HBEA(50-50)	0.045	20	0.70	3.7	0.13	0.46	0.41
	PtA-HBEA(75-25)	0.130	21	0.47	3.7	0.14	0.53	0.32

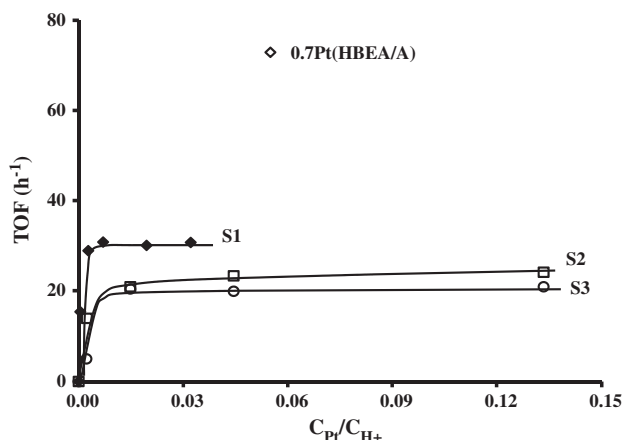


Fig. 2. Turn-over frequency (TOF) of the acid sites versus C_{Pt}/C_{H+} ratio.

change in these TOF values vs. the balance between hydrogenating and acid functions expressed by the ratio between the concentrations of accessible Pt atoms and protonic sites (C_{Pt}/C_{H+}) is reported in Fig. 2. Whatever the catalyst series, the hydroisomerization activity increases significantly at low C_{Pt}/C_{H+} values and then remains constant; furthermore, for identical C_{Pt}/C_{H+} values, TOF decreases from S1 to S2 then to S3 catalysts, hence decreases with the degree of intimacy between hydrogenating and acid functions.

However, the shape of the curves in Fig. 2 is independent of the platinum location (on zeolite or on alumina): significant TOF increase at low values of C_{Pt}/C_{H+} , then a plateau or a quasi-plateau. This shape of curve which is classically observed in bifunctional catalysis [4,8–10] can be explained by a change in the rate limiting reaction, catalyzed by the platinum sites: at low C_{Pt}/C_{H+} values and by the acid sites, at high values. Nevertheless, with the exchanged PtHBEA samples (S1), the plateau was obtained at lower C_{Pt}/C_{H+} values and the TOF values were higher (~1.5 times) than with the PtA-HBEA composite catalysts (Fig. 3). Lastly, the TOF of the 0.7Pt/(HBEA/A) catalyst was found to be ~2.5 times greater than the TOF of Pt/HBEA samples (Table 2 and Fig. 2).

Monobranched isomers (M), bi- and multibranched isomers (B), and cracking products (C) were formed over all the bifunctional catalysts. However, the product distribution depended on the catalyst and on the degree of n -C₁₆ conversion. This is shown for the three series of catalysts in Fig. 3a–c in which the yield in isomers is plotted vs. n -C₁₆ conversion (X). When, at low X values, the experimental curve follows the dotted line which corresponds to a totally selective formation of isomers from n -C₁₆, this means that only isomers appear as primary products, C products resulting from the secondary transformation of isomers, i.e., that the scheme of n -C₁₆ transformation is successive: n -C₁₆ \rightleftharpoons I \rightarrow C.

It is what can be observed for the 0.7Pt/(HBEA/A) catalyst chosen as reference (Fig. 3a). In contrast, with all the other catalysts, even at very low n -C₁₆ conversion, no experimental points were located on the dotted line; this means that at least part of the cracking products (C) result apparently from the direct transformation of n -C₁₆. The significance of this apparent direct formation of C from n -C₁₆ can be qualitatively estimated from the distance between the experimental curves and the dotted line. However, this significance can be quantitatively expressed by the initial value of the cracking/isomers yield ratio (C/I) drawn by extrapolation at zero conversion of the (C/I) vs. X curve (Fig. 4a–c).

The same type of plot was used to estimate the initial (i.e., by extrapolation at $X=0$) value of the (B/M) ratio between the yields in multi- and monobranched isomers (Fig. 4d–f). Again this initial B/M ratio was equal to zero with the reference

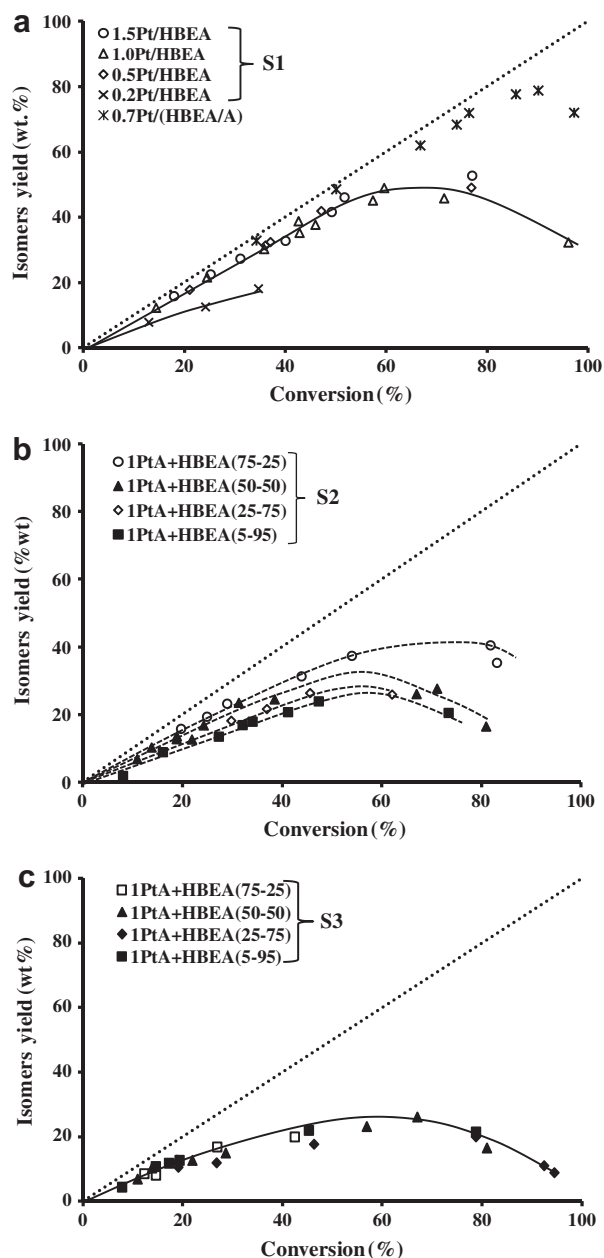


Fig. 3. Yield in isomers vs. n -C₁₆ conversion for the three series of bifunctional catalysts: (a) Pt/HBEA (S1) and 0.7Pt/(HBEA/A) catalysts, (b) S2: intimate mixture of PtA and HBEA, (c) S3: physical mixture of PtA and HBEA.

catalyst 0.7Pt/(HBEA/A) only, which means that on this catalyst n -hexadecane transformation occurred via a perfectly successive scheme:



With all the other catalysts, part of B and C appeared as primary products, the other part resulting from secondary transformation.

The initial (i.e., at zero conversion) values of the C/I and B/M ratio, drawn from Fig. 4, are reported in Table 2 and moreover plotted as a function of the C_{Pt}/C_{H+} ratio in Fig. 5a and b. This Fig. 5 shows that, as was the case for the TOF values (Fig. 2), these ratios depended significantly on both the balance between hydrogenating and acid functions (C_{Pt}/C_{H+}) and on the degree of intimacy between acid and platinum sites: Thus for identical C_{Pt}/C_{H+} values, the initial C/I and B/M ratios decrease when the intimacy between Pt and

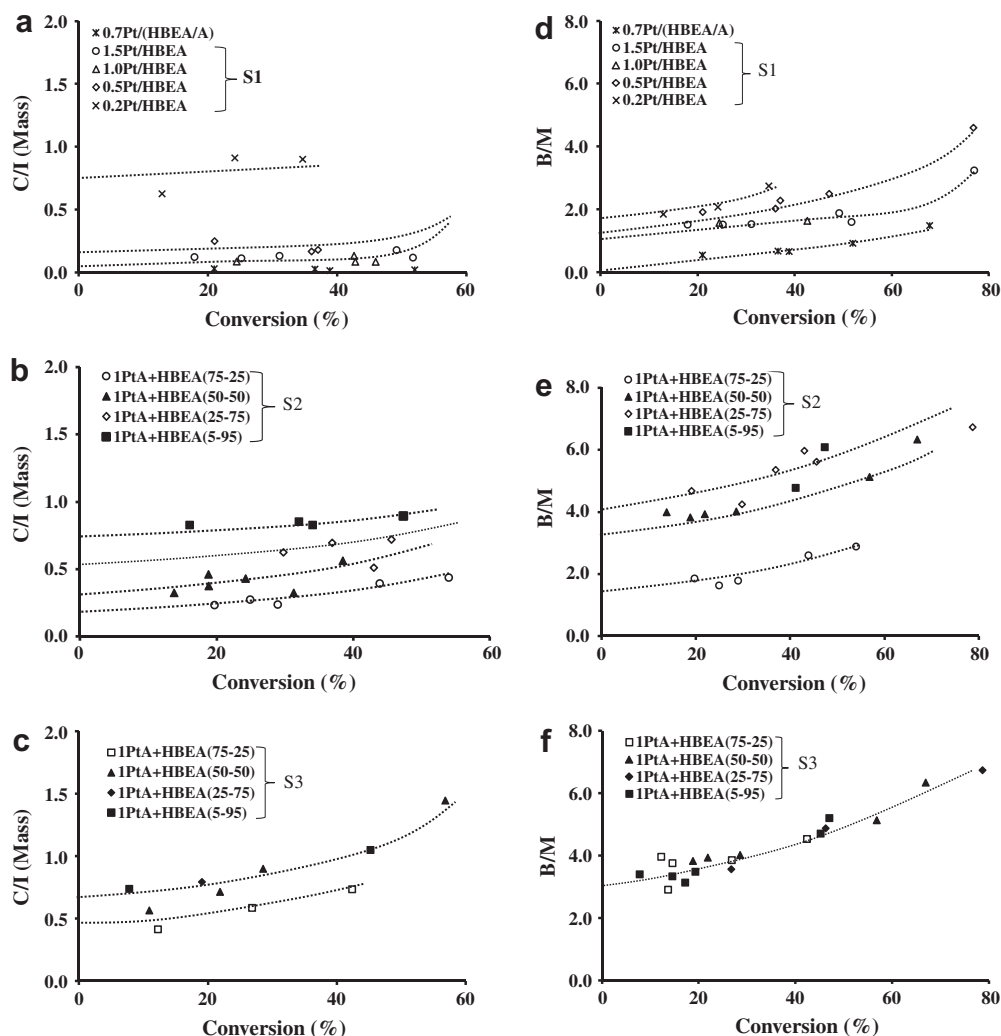


Fig. 4. Ratio between the wt% ratio of the cracking/isomer ratio (C/I) and of the multibranched and monobranched isomers (B/M) vs. n -C₁₆ conversion; (a and d) Pt/HBEA (S1) and 0.7Pt/(HBEA/A) catalysts, (b and e) S2: intimate mixture of PtA and HBEA, (c and f) S3: physical mixture of PtA and HBEA.

protonic sites increases, i.e., from S3 to S2 then to S1. It can therefore be concluded that for getting a perfectly successive scheme, at least two conditions had to be satisfied: enough high C_{Pt}/C_{H+} values and high degree of intimacy between hydrogenating and acid functions. The initial C/I and B/M values were used for estimating the initial product distributions; these distributions are reported in Table 2.

With all the bifunctional catalysts, cracking products (C) were essentially constituted of C₃–C₁₃ linear and branched products. The absence of methane and the very low amount of ethane in the C products suggests that hydrogenolysis reactions over Pt sites can be neglected. For all the catalysts of series 1, 2 and 3, the molar distributions of the C products, estimated at low n -C₁₆ conversion into C products, were plotted in Fig. 6a–c as a function of the number of carbons atoms (n_C). Two main types of distribution profile can be distinguished. The first one, nearly flat, observed with most of the samples of series 1 and 2 is that expected from a primary cracking process. The second one, with two maxima at 4 C and 11–12 C atoms, shows that the products of primary cracking undergo secondary transformations, either dimerization or cracking, as the maximum at 4 C atoms is less pronounced (0.7Pt/(HBEA/A) catalyst) or more pronounced (S3 catalysts, plus those of series 1 and 2 with the lowest C_{Pt}/C_{H+} values) than the maximum at 11–12

C atoms. This classification of the catalysts is confirmed from the values of the molar C_4/C_{12} and C_5/C_{11} ratios, close to 1 in absence of secondary transformations of cracking products, lower or higher than 1 when the primary cracking is followed by dimerization or secondary cracking (Table 3). The degree of secondary cracking (%Cs) or dimerization was estimated from the number of C molecules formed per molecule of cracked n -C₁₆ molecule (N_C). The N_C and C_s values are reported in Table 3. As could be expected, N_C values higher than 2 (≥ 2.3) were found in presence of secondary cracking, i.e., with all the S3 samples and with the samples of series 1 and 2 with the lowest C_{Pt}/C_{H+} values.

With all the catalysts, the heavy C products were found to be essentially branched: thus, in C₁₀ and C₁₁ products, the branched/linear ratios were between 6 and 12. Furthermore, while C₄ and C₅ products were essentially branched (branched/linear ratios of 6–7) with all the S3 catalysts and with the samples of series 2 with the lowest C_{Pt}/C_{H+} values, linear products became preponderant with the other samples, particularly in the C₄ fraction. Thus, with all the S1 samples and the 50-50 and 75-25 S2 samples, the branched/linear ratios were close to 1 in C₅ products and between 0.1 and 0.3 in C₄ products. This difference in branching between light and heavy cracking products suggests a fast secondary skeletal isomerization of the heavy C products and practically no

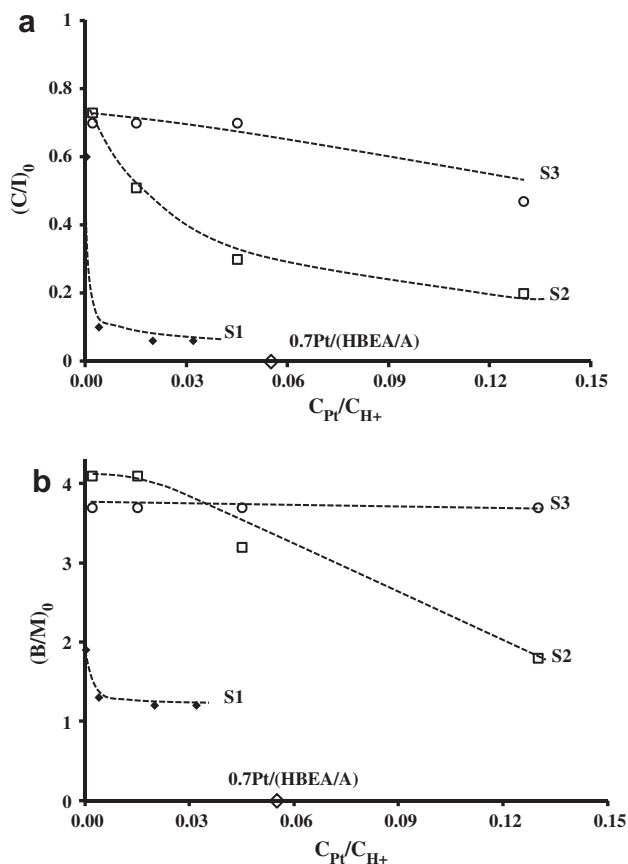


Fig. 5. Initial values of the wt% ratio of the cracking/isomer ratio $(C/I)_0$ (a) and of the multibranched and monobranched isomers $(B/M)_0$ (b) vs. C_{Pt}/C_{H^+} . Pt/HBEA (S1) and 0.7Pt/(HBEA/A) catalysts, intimate (S2) and physical (S3) mixtures of PtA and HBEA.

skeletal isomerization of linear C_5 and especially C_4 products. The absence of secondary isomerization in C_4 products could be related to the fact that very unstable primary carbenium ions are involved as intermediates in the monomolecular isomerization of C_4 hydrocarbons [38].

4. Discussion

As it is well known, the balance between the hydrogenating and acid functions of the bifunctional catalysts determines for a large part their catalytic properties. This was quantitatively shown for the first time in n -heptane (n - C_7) and n -decane (n - C_{10}) transformation over a series of Pt-exchanged USHY catalysts [21–24] that the ratio between the concentrations of accessible Pt atoms and acid sites (C_{Pt}/C_A) being chosen to express quantitatively the hydrogenating/acid balance. The determining effect of this balance is confirmed here in n - C_{16} hydroisomerization over three series of bifunctional Pt-HBEA catalysts differing by the degree of intimacy between hydrogenating and acid functions. As olefin skeletal rearrangement and cracking are catalyzed by the protonic acid sites only, the ratio between the concentrations of accessible Pt atoms and acid sites (C_{Pt}/C_A) was substituted by C_{Pt}/C_{H^+} . In each of the three catalyst series, the activity per protonic acid site (TOF) was shown to increase firstly with the hydrogenating/acid balance and then to become practically constant. This change is typical of a bifunctional catalytic process with, at low C_{Pt}/C_{H^+} values, limitation of the rate of n - C_{16} transformation by the hydro/dehydrogenation steps over the Pt sites and at high values by the rearrangement of olefinic intermediates over the protonic sites.

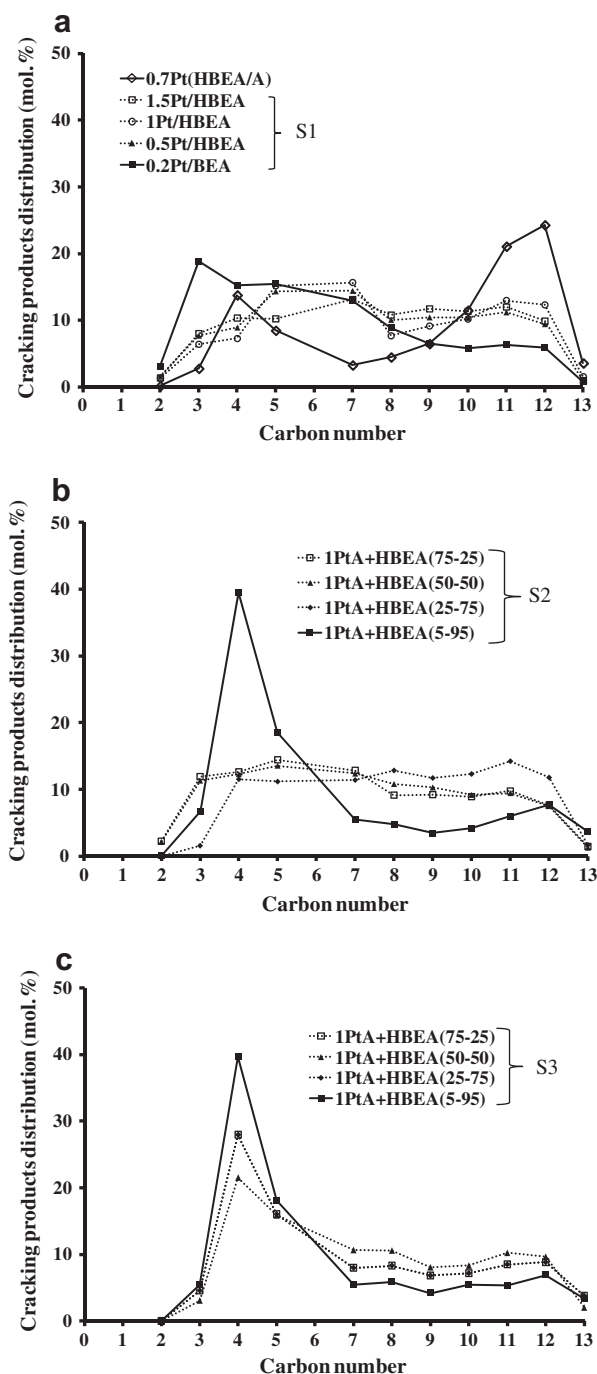


Fig. 6. Cracking product distribution (mol.%): percentage of cracking products as a function of the number of their carbon atoms. (a) Pt/HBEA (S1) and 0.7Pt/(HBEA/A) catalysts, (b) S2: intimate mixture of PtA and HBEA, (c) S3: physical mixture of PtA and HBEA.

However, the difference in TOF and in product distribution between the three catalyst series (Figs. 2–5) which can be observed for identical C_{Pt}/C_{H^+} values demonstrates that the bifunctional process was also affected by at least one additional physicochemical characteristic of the bifunctional catalysts. This proposal is confirmed by the observation that the selectivity to isomers, especially to monobranched isomers M continues to increase above the C_{Pt}/C_{H^+} values required for getting the optimal value of the activity per protonic acid site (TOF). Both observations suggest that the average degree of intimacy between active Pt and protonic sites

Table 3
Initial values at low n -C₁₆ conversion into cracking products of the C₄/C₁₂ and C₅/C₁₁ molar ratios in the cracking products. Values of N_C, the number of cracking molecules per molecule of cracked n -C₁₆, estimated from the product distribution and percentage (%C_S) of secondary cracking.

Series	Catalyst	X _C (%)	C ₄ /C ₁₂	C ₅ /C ₁₁	N _C ^a	%C _S
S1	0.7Pt/(HBEA/A)	5	0.6	0.4	1.6	20 ^b
	0.2Pt/HBEA	5	2.5	2.4	2.65	33
	0.5Pt/HBEA	5	0.8	1.4	2.15	8
	1.0Pt/HBEA	5	0.6	1.2	2.25	13
	1.5Pt/HBEA	5	1.0	0.9	2.00	0
S2	PtA-HBEA(5-95)	5	5.2	3.1	2.5	25
	PtA-HBEA(25-75)	12	1.0	0.8	2.00	0
	PtA-HBEA(50-50)	7	1.6	1.4	1.95	0
	PtA-HBEA(75-25)	6	1.7	1.5	1.95	0
	PtA-HBEA(5-95)	7	5.8	3.4	2.6	30
S3	PtA-HBEA(25-75)	28	3.2	1.9	2.3	15
	PtA-HBEA(50-50)	9	2.2	1.5	2.25	13
	PtA-HBEA(75-25)	10	3.2	1.9	2.3	15

^a Estimated by considering the molar concentration of C₆ molecules as equal to half of the sum of the C₅ and C₇ products concentration.

^b With this catalyst, %C_S is the percentage of dimerization.

Table 4
Estimation of n_{as} , the average number of acid steps involved in the transformation of one molecule of n -C₁₆ and TOF_{cor} values (number of acid steps per protonic acid site and per hour).

Series	Catalyst	M	B	C	n_{as}	TOF _{cor}
S1	0.7Pt/(HBEA/A)	1	0	0	1	73
	0.2Pt/HBEA	0.22 ^a	0.41 ^a × 2.5 ^b = 1.02	0.37 ^a × 4.33 ^c = 1.60	2.84	43
	0.5Pt/HBEA	0.40 ^a	0.51 ^a × 2.5 ^b = 1.28	0.09 ^a × 4.08 ^c = 0.37	2.05	64
	1.0Pt/HBEA	0.43 ^a	0.51 ^a × 2.5 ^b = 1.28	0.06 ^a × 4.13 ^c = 0.25	1.96	59
	1.5Pt/HBEA	0.43 ^a	0.51 ^a × 2.5 ^b = 1.28	0.06 ^a × 4.00 ^c = 0.24	1.95	60
S2	PtA-HBEA(5-95)	0.11 ^a	0.46 ^a × 2.5 ^b = 1.15	0.42 ^a × 4.25 ^c = 1.79	3.05	43
	PtA-HBEA(25-75)	0.13 ^a	0.53 ^a × 2.5 ^b = 1.33	0.34 ^a × 4.00 ^c = 1.36	2.82	59
	PtA-HBEA(50-50)	0.18 ^a	0.59 ^a × 2.5 ^b = 1.48	0.23 ^a × 4.00 ^c = 0.92	2.58	59
	PtA-HBEA(75-25)	0.30 ^a	0.54 ^a × 2.5 ^b = 1.35	0.17 ^a × 4.00 ^c = 0.68	2.33	56
	PtA-HBEA(5-95)	0.13 ^a	0.46 ^a × 2.5 ^b = 1.15	0.41 ^a × 4.30 ^c = 1.77	3.05	15
S3	PtA-HBEA(25-75)	0.13 ^a	0.46 ^a × 2.5 ^b = 1.15	0.41 ^a × 4.16 ^c = 1.71	2.99	63
	PtA-HBEA(50-50)	0.13 ^a	0.46 ^a × 2.5 ^b = 1.15	0.41 ^a × 4.13 ^c = 1.70	2.98	60
	PtA-HBEA(75-25)	0.14 ^a	0.53 ^a × 2.5 ^b = 1.33	0.32 ^a × 4.15 ^c = 1.33	2.80	59

^a Wt fractions of monobranched (M), multibranched (B) isomers and cracking products (C).

^b Number of acid steps involved in the apparent transformation of one molecule of n -C₁₆ into B product.

^c Number of acid steps involved in the apparent transformation of one molecule of n -C₁₆ into C product.

is most likely the additional determining physicochemical characteristics of the bifunctional catalysts.

Large differences in the hydrogenating/acid balance (expressed by the C_{Pt}/C_A values) required for getting optimal values of the activity per protonic acid site (TOF) and of stability and selectivity had been previously observed in n -C₇ and n -C₁₀ transformation on a series of Pt-exchanged USHY. To explain this observation, the additional determining parameter was proposed to be the average number of acid sites n_{as} , responsible for the rearrangement and cracking of the olefinic intermediates along their diffusion between two Pt sites [39]. It was also advanced that for getting optimal catalytic characteristics ("ideal" bifunctional catalysis), two conditions had to be satisfied: C_{Pt}/CH₊ values high enough so that the acid catalyzed reactions be rate-limiting and number of acid sites between two Pt sites low enough to catalyze only one step of skeletal rearrangement (with additional branching) or cracking of olefinic intermediates [40].

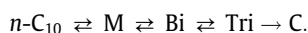
Unfortunately, the value of n_{as} cannot be easily determined from the physicochemical characteristics of the bifunctional catalysts. Indeed while the concentration of protonic sites of the BEA component is known, the characteristics of the diffusion path of olefinic intermediates are difficult to be established and moreover the probability that the protonic sites have to be active under the operating conditions cannot be specified. However, as with all

the catalysts, the same HBEA zeolite was used as acid component and the number of protonic sites that olefinic intermediates can encounter along their diffusion within the BEA micropores between Pt sites can be considered as proportional to the distance they travel through the BEA zeolite between these sites, i.e., their path of diffusion. This distance d depends on two main parameters: the mode of combination between the metal and acid functions (series 1–3) and the ratio between the concentrations of accessible Pt and protonic sites (C_{Pt}/C_{H+}). Another parameter which cannot be considered here is that within the tridimensional micropore system of the BEA zeolite, molecular diffusion is tridirectional; however, as the same zeolite sample was used, the d values estimated below will be proportional to the actual d values, hence to the total number of protonic acid sites located on the diffusion path of olefinic intermediates. With the S₁ catalysts, Pt is essentially located on the outer surface of the zeolite agglomerates and the distance d between Pt sites corresponds at least to the size (~12.5 μm) of these agglomerates. With the composite catalysts of series 3, d corresponds at least to the size of the zeolite particles, i.e., ~300 μm ø. With those of series 2, d changes with the catalyst composition and the simplest way to approximate this distance is to multiply the diameter of the catalyst particle (~300 μm ø) by the percentage of the HBEA component in the catalyst. Therefore, for identical C_{Pt}/C_{H+} values, e.g., at the activity plateau, d , hence

n_{as} should increase from S1 to S2 then to S3 catalysts, thus with the decrease in the intimacy between metal and acid sites.

To overcome the difficulty of a quantitative estimation of n_{as} , a simple method based on experimental catalytic data was recently proposed [39]. Firstly, it can be remarked that this average number of active acid sites encountered by the olefinic intermediates along their diffusion between two Pt sites (n_{as}) is equal to the number of acid rearrangement or cracking steps involved in the transformation of one reactant molecule [39]. n_{as} can therefore be estimated from the product distribution extrapolated at zero conversion, provided however to know the number of acid steps required for the apparent direct formation of each of the product molecules from $n\text{-C}_{16}$.

The method used for estimating n_{as} was based on the conclusions of the modelling of n -decane transformation over an “ideal” bifunctional PtHFAU catalyst [23], namely that this transformation could be considered to occur through the following simple successive scheme:



Indeed, cracking products (C) were found to be essentially formed from multibranched isomers and mainly through the tribranched isomers (Bi) [23]. A similar conclusion can be drawn from the relative rates of product formation during $n\text{-C}_{16}$ transformation over a Pt/HBEA catalyst, estimated from the application of the single event microkinetic model [41]. Therefore, in this paper, the bifunctional hydrocracking of $n\text{-C}_{16}$, monobranched (M) and even bibranched (Bi) isomers were neglected in comparison with the hydrocracking of tribranched (Tri) isomers. Hence, whereas only one single step of acid transformation of olefinic intermediates ($n\text{-C}_{16}^+ \rightarrow \text{M}^+$) is involved in the formation of M from $n\text{-C}_{16}$, two, three, and four acid successive steps are requested for the apparent direct formation of Bi, Tri, and primary C products from $n\text{-C}_{16}$. However, whereas in $n\text{-C}_{10}$ transformation over the PtHFAU catalysts, secondary cracking could be neglected [23], this reaction was shown to exist over all the catalysts of series 3 and on those of series 1 and 2 with low C_{Pt}/C_{H^+} values (Table 3). Therefore, this secondary cracking has to be considered in the estimation of n_{as} , which was made with the logical assumption that five acid steps were involved in the formation of the corresponding products.

The determination of n_{as} is detailed in Table 4 for all the catalysts: n_{as} is simply the sum of the products of the weight fractions of M, B, and C by the average number of acid reactions required from their formation from $n\text{-C}_{16}$, i.e., 1 for M, 2.5 for B (the ratio between bi- and tribranched isomers being close to 1 with all the catalysts) and between 4 and 4.33 for C, depending of the percentage (%Cs) of secondary cracking reported in Table 3. It should however be remarked that if a unique relationship between product yields and total conversion can be obtained under “ideal” hydrocracking conditions (e.g., for $n_{as} = 1$), this is not the case under nonideal conditions with a significant effect of operating temperature and pressure on the product distribution [20]. Therefore, the n_{as} values reported in Table 4 are only valid under the conditions of this work.

Table 4 and Fig. 7a show that with all the S₃ catalysts, the n_{as} values were close to 3, while with the catalysts of S1 and S2 series, n_{as} decreases with the increase in C_{Pt}/C_{H^+} ; however, at identical C_{Pt}/C_{H^+} , the n_{as} values were lower in series 1 and their decrease with the C_{Pt}/C_{H^+} increase more pronounced than in series 2. Therefore, as demonstrated above, the greater the distance between Pt sites, the higher the n_{as} value. This is shown in Fig. 7b in which the n_{as} values at the plateau of TOF_{cor} (i.e., when hydroisomerization is limited by acid steps) are plotted as a function of the estimated d values. The effect of d on n_{as} is particularly pronounced at low d values, n_{as} increasing from 1 (i.e., its minimum value) for $d = 0.04 \mu\text{m}$ to 2 for $d = 12.5 \mu\text{m}$, the increase in d from 12.5 to 300 μm causing the same increase in one unit only.

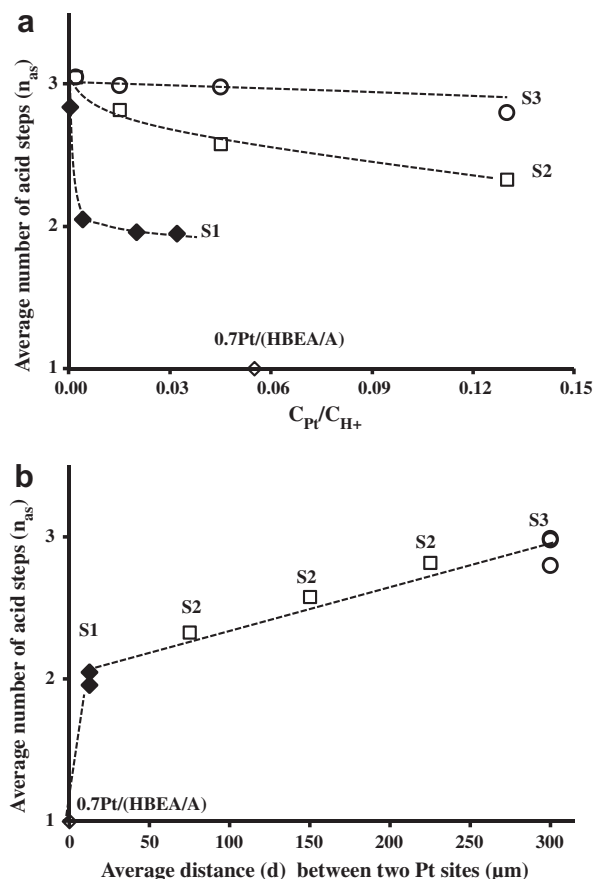


Fig. 7. Average number of acid steps (n_{as}) involved in the transformation of one $n\text{-C}_{16}$ molecule vs. the C_{Pt}/C_{H^+} ratio (a) and vs. the distance (d , μm) between two platinum sites (b).

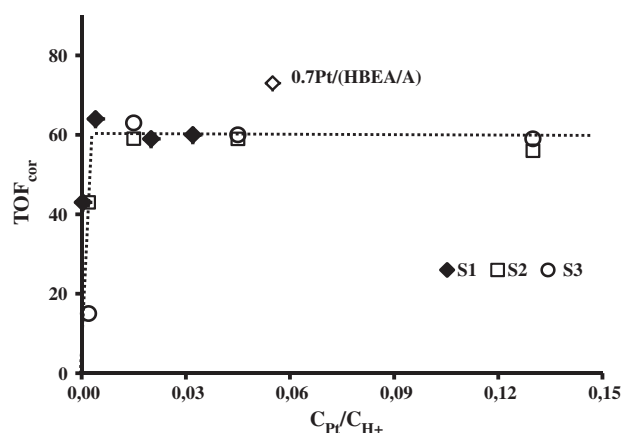


Fig. 8. Corrected values of the turnover frequency TOF_{cor} (number of acid steps per protonic site and per hour) vs. the C_{Pt}/C_{H^+} ratio.

In order to take into account the necessity of more than one acid step for the direct production from $n\text{-C}_{16}$ of multibranched (Bi, Tri, etc.) isomers and primary and secondary C products, corrected values of the turnover frequency (TOF_{cor}) of the acid sites were calculated by multiplying the apparent TOF values expressed in molecules of $n\text{-C}_{16}$ converted per acid sites and per hour (Table 2) by n_{as} , the average number of acid steps per molecule of $n\text{-C}_{16}$ converted. This means that the TOF_{cor} values are expressed as the number of acid steps (skeletal rearrangement or cracking)

undergone by the olefinic intermediates ($n\text{-C}_{16}^-$) per protonic acid site and per hour. Nearly, similar TOF_{cor} values were obtained with all the catalysts except the one with the smallest $C_{\text{Pt}}/C_{\text{H}^+}$ value (0.0003), a quasi plateau being obtained for $C_{\text{Pt}}/C_{\text{A}} \geq 0.004$ (Fig. 8).

The most important observation is that identical TOF_{cor} values were obtained with the three series of catalysts, hence that the activity of bifunctional catalysts in n -alkane transformation depends on two parameters only: (i) the balance between the hydrogenating and acid functions ($C_{\text{Pt}}/C_{\text{H}^+}$) and (ii) the number n_{as} of acid steps undergone by olefinic intermediates during their diffusion from the Pt sites on which they are formed up to those on which they are rehydrogenated. It should however be remarked that with the “ideal” 0.7 wt% Pt(HBEA/A) catalyst used in previous studies [36,37], the n_{as} value of which is equal to 1 (hence $\text{TOF}_{\text{cor}} = \text{TOF}$) and the TOF_{cor} value was 14% higher than that obtained at the activity plateau with the catalysts of series S1, 2, and 3. This difference could be related to the approximations which were made in the determination of the n_{as} values, owing to imperfections in the quantitative analysis of multibranched isomers and of the secondary cracking products. It could also be due to the difference in rate constants of isomerization and cracking of olefinic intermediates, greater for cracking of tribranched intermediates than those of isomerization (from linear to monobranched, mono- to bi-branched, and bi- to tribranched intermediates) [23]. However, this last explanation does not seem valid, for similar high values of corrected TOF should be obtained with the S1 catalysts with high $C_{\text{Pt}}/C_{\text{H}^+}$ ratio on which the initial formation of cracking products is very limited, which is not the case. The most likely explanation [36,37] is that the higher efficiency (and selectivity) of this composite catalyst is related to the easier diffusion of the olefinic intermediates within, hence desorption from, the micropores of the nanocrystals of its HBEA component.

Another important observation is that, like in $n\text{-C}_{10}$ transformation over PtHFAU catalysts [39], a very low value of $C_{\text{Pt}}/C_{\text{H}^+}$ (0.004) is enough to obtain the TOF_{cor} plateau, which means that one Pt site is able to feed a very large number of protonic sites (~ 250) with olefinic intermediates. This suggests that a low content of well-dispersed Pt is enough for obtaining optimal activity, stability, and selectivity to isomers (“ideal” bifunctional catalysis).

5. Conclusions

n -Hexadecane ($n\text{-C}_{16}$) transformation was studied over a large range of conversion, on three series of bifunctional catalysts with Pt and HBEA as hydro-dehydrogenating and acid components, with large differences in the degree of components intimacy: series 1 with Pt located on the outer surface of HBEA crystal agglomerates of $\sim 12.5 \mu\text{m}$, series 2 and 3 of composite catalysts formed by combination of $\text{Pt-Al}_2\text{O}_3$ and HBEA particles of $\sim 70 \mu\text{m}$ (series 2) or resulting from the mechanical mixture of $\text{Pt-Al}_2\text{O}_3$ and HBEA particles of $\sim 300 \mu\text{m}$.

In the three series, the activity and the selectivity of the catalysts were shown to be dependent on the balance between hydrogenating and acid functions expressed by the $C_{\text{Pt}}/C_{\text{H}^+}$ ratio of the concentrations of accessible Pt atoms and protonic acid sites. Thus, in each of the series, the activity per protonic acid site (TOF) was shown to increase firstly with $C_{\text{Pt}}/C_{\text{H}^+}$ and then to become practically constant. A significant change in the product distribution with $C_{\text{Pt}}/C_{\text{H}^+}$ could also be observed, and the bifunctional process becoming more and more selective to isomers, especially to monobranched ones with the increase in $C_{\text{Pt}}/C_{\text{H}^+}$.

However, two observations show that the balance between hydrogenating and acid functions is not the only parameter determining the catalytic properties: (i) the difference in TOF and in product distribution between the three catalyst series observed

for identical $C_{\text{Pt}}/C_{\text{H}^+}$ values and (ii) the increase in the selectivity to isomers above the $C_{\text{Pt}}/C_{\text{H}^+}$ values required for getting the optimal TOF value. Considering the large difference in the degree of intimacy of active Pt and protonic sites between the three series of catalysts, this characteristic was proposed to be the additional determining parameter. Unfortunately, this parameter cannot be easily quantified from the physicochemical characteristics of the bifunctional catalysts. This has led us to substitute it by another parameter, i.e., the number of acid steps (n_{as}) undergone by olefinic intermediates in the initial (estimated at zero conversion) transformation of each molecule of $n\text{-C}_{16}$, which can be drawn from the initial product distributions.

The calculated n_{as} values were used to estimate corrected values of TOF (TOF_{cor}), which were shown to be similar for the three series of catalysts. This similarity in TOF_{cor} values demonstrates that both the activity and selectivity of the bifunctional Pt-HBEA catalysts depend on only two parameters easy to be quantified: the balance between hydrogenating and acid functions and the degree of intimacy between the corresponding sites. This important conclusion allows to reject the alternative proposals proposed to explain the behavior of bifunctional Pt-H zeolite catalysts, in particular that of a positive effect of hydrogen spillover from the metal to the acid sites.

Moreover, although the essential role played in bifunctional catalysis by the degree of intimacy between the hydro-dehydrogenating and protonic acid sites is re-known from a long time [4], no direct and accurate method for estimating this parameter from the physicochemical characteristics of catalysts has been yet developed. The n_{as} parameter proposed here whose estimation in chosen model reactions is very simple can therefore be considered as an attractive tool for characterizing this degree of intimacy in various bifunctional catalysts and for designing optimal (“ideal”) industrial catalysts for complex processes.

Acknowledgment

Ludovic Pinard thanks IFPEN for its financial support.

References

- [1] R.H. Jensen, in: M. Guisnet, J.P. Gilson (Eds.), *Zeolites for Cleaner Technologies*, Catalytic Science Series, vol. 3, Imperial College Press, 2002, p. 75 (Chapter 4).
- [2] M. Daage, in: M. Guisnet, J.P. Gilson (Eds.), *Zeolites for Cleaner Technologies*, Catalytic Science Series, vol. 3, Imperial College Press, 2002, p. 167 (Chapter 8).
- [3] C. Bouchy, G. Hastoy, E. Guillon, J.A. Martens, *Oil Gas Sci. Technol. – Rev. IFP* 64 (2009) 91.
- [4] P.B. Weisz, *Adv. Catal.* 13 (1962) 137.
- [5] J. Weitkamp, *Erdöl Kohle Erdgas Petrochem.* 31 (1978) 13.
- [6] J. Weitkamp, S. Ernst, in: D. Barthomeuf, E.G. Derouane, W. Hölderich (Eds.), *Guidelines for Mastering the Properties of Molecular Sieves*, NATO ASI Series B, vol. 221, 1990, p. 343.
- [7] J. Weitkamp, *ChemCatChem* 4 (2012) 292.
- [8] M. Guisnet, G. Perot, in: F.R. Ribeiro et al. (Eds.), *Zeolites: Science and Technology – NATO ASI Series*, Martinus Nijhoff Publishers, The Hague, Boston, Lancaster, 1984, p. 397.
- [9] M. Guisnet, *Polish J. Chem.* 77 (2003) 637.
- [10] C. Marciilly, *Catalyse acido-basique, Application au raffinage et à la pétrochimie*, vol. 1, Eds. Technip, Paris, 2004 (Chapter 4).
- [11] F. Roessner, U. Roland, *J. Mol. Catal. A* 112 (1996) 401.
- [12] U. Roland, T. Braunschweig, F. Roessner, *J. Mol. Catal. A* 127 (1997) 61.
- [13] A. Zhang, I. Nakamura, K. Aimoto, K. Fujimoto, *Ind. Eng. Chem. Res.* 34 (1995) 1074.
- [14] T. Kusakari, K. Tomishige, K. Fujimoto, *Appl. Catal. A* 224 (2002) 219.
- [15] R. Prins, *Chem. Rev.* 112 (2012) 2714.
- [16] J. Weitkamp, *Ind. Eng. Chem. Prod. Res. Dev.* 21 (1982) 550.
- [17] J.A. Martens, P.A. Jacobs, J. Weitkamp, *Appl. Catal.* 20 (1986) 239.
- [18] J.A. Martens, P.A. Jacobs, J. Weitkamp, *Appl. Catal.* 20 (1986) 283.
- [19] G.G. Martens, G.B. Marin, J.A. Martens, P.A. Jacobs, G.V. Baron, *J. Catal.* 195 (2000) 253.
- [20] J.W. Thybaut, C.S. Laxmi Narasimhan, J.F. Denayer, G.V. Baron, P.A. Jacobs, J.A. Martens, G.B. Marin, *Ind. Eng. Chem. Res.* 44 (2005) 5159.
- [21] G.E. Giannetto, G.R. Pérot, M. Guisnet, *Ind. Eng. Chem., Prod. Res. Dev.* (1986) 481.
- [22] M. Guisnet, F. Alvarez, G. Giannetto, G. Perot, *Catal. Today* 1 (1987) 415.

- [23] F. Alvarez, F.R. Ribeiro, G. Pérot, C. Thomazeau, M. Guisnet, *J. Catal.* 162 (1996) 179.
- [24] G. Giannetto, F. Alvarez, F.R. Ribeiro, G. Perot, M. Guisnet, in: D. Barthomeuf, E.G. Derouane, W. Hölderich (Eds.) *Guidelines for Mastering the Properties of Molecular Sieves*, NATO ASI Series B, vol. 221, 1990, p. 355.
- [25] T. Yashima, Z.B. Wang, A. Kamo, T. Yoneda, T. Komatsu, *Catal. Today* 29 (1996) 279.
- [26] A. Lugstein, A. Jentys, H. Vinek, *Appl. Catal. A* 166 (1998) 29.
- [27] A. Soualah, J.L. Lemberon, L. Pinard, M. Chater, P. Magnoux, K. Moljord, *Appl. Catal. A* 336 (2008) 23.
- [28] J.A. Martens, R. Parton, L. Uytterhoeven, P.A. Jacobs, G.F. Froment, *Appl. Catal.* 76 (1991) 95.
- [29] J.A. Martens, P.A. Jacobs, in: E.G. Derouane et al. (Eds.), *Zeolite Microporous Solids: Synthesis, Structure and Reactivity*, NATO ASI Series C, vol. 352, 1992, p. 511.
- [30] J.A. Martens, W. Souverijns, W. Verrelst, R. Parton, G.F. Froment, P.A. Jacobs, *Angew. Chem. Int. Ed. Engl.* 34 (1995) 22.
- [31] M. Guisnet, *J. Mol. Catal.* 182–183 (2002) 364.
- [32] N. Batalha, A. Soualah, L. Pinard, Y. Pouilloux, F. Lemos, T. Belin, *J. Chromatogr. A* 1260 (2012) 206.
- [33] M. Guisnet, P. Ayrault, J. Datka, *Polish J. Chem.* 71 (1997) 1455.
- [34] C. Binet, A. Jadi, J.C. Lavalley, *J. Chim. Phys.* 86 (3) (1989) 451.
- [35] J.F. Lepage, in: *Catalyse de contact*, Eds. Technip 1968, Paris (Chapter 2).
- [36] N. Batalha, S. Morisset, L. Pinard, I. Maupin, J.L. Lemberon, F. Lemos, Y. Pouilloux, *Microporous Mesoporous Mater.* 166 (2013) 161.
- [37] N. Batalha, L. Pinard, S. Morisset, J.L. Lemberon, Y. Pouilloux, M. Guisnet, F. Lemos, F.R. Ribeiro, *React. Kinet., Mech. Catal.* 107 (2012) 285.
- [38] G. Caeiro, R.H. Carvalho, Y. Wang, M.A.N.D.A. Lemos, F. Lemos, M. Guisnet, F. Ramôa Ribeiro, *J. Mol. Catal. A* 255 (2006) 131.
- [39] N. Batalha, L. Pinard, Y. Pouilloux, M. Guisnet, *Catal. Lett.* 143 (6) (2013) 587.
- [40] M. Guisnet, *Catal. Today*, doi: <http://dx.doi.org/10.1016/j.cattod.2013.04.028>.
- [41] B.D. Vandegehuchte, J.W. Thybaut, A. Martinez, M.A. Arribas, G.B. Marin, *Appl. Catal. A* 441–442 (2012) 10.